All-polarization-maintaining, polarization-multiplexed, dual-comb fiber laser with a nonlinear amplifying loop mirror

doi: 10.1364/OE.27.014648

Research Article | Vol. 27, No. 10 | 13 May 2019 | OPTICS EXPRESS 14648
Optics EXPRESS

All-polarization-maintaining, polarization-multiplexed, dual-comb fiber laser with a nonlinear amplifying loop mirror

YOSHIAKI NAKAJIMA,[1,2] YUYA HATA,[1,2] AND KAORU MINOSHIMA[1,2,*]

[1]*Department of Engineering Science, Graduate School of Informatics and Engineering, University of Electro-Communications, 1-5-1 Chofugaoka, Chofu, Tokyo 182-8585, Japan*
[2]*Japan Science and Technology Agency (JST), Exploratory Research for Advanced Technology (ERATO), MINOSHIMA Intelligent Optical Synthesizer (IOS) Project, 1-5-1 Chofugaoka, Chofu, Tokyo 182-8585, Japan*
**k.minoshima@uec.ac.jp*

Abstract: We developed an all-polarization-maintaining, polarization-multiplexed, dual-comb fiber laser with a nonlinear amplifying loop mirror (NALM) mode-locking mechanism. Owing to the use of the slow and fast axes of a polarization-maintaining fiber (PMF), the dual-frequency combs with slightly different repetition rates from the single-laser cavity are generated at the same center wavelength without extra-cavity nonlinear spectral broadening. The narrow relative beat note between the two frequency combs is obtained with a full-width-at-half-maximum of ~1 kHz in the optical frequency domain. The two frequency combs have high relative stability and mutual coherence owing to passive common-mode noise cancellation.

1. Introduction

Optical frequency combs have become indispensable tools in various scientific and technical fields, such as frequency metrology, high-precision spectroscopy, high-precision microwave generation, optical communication, arbitrary waveform generation, astronomical spectrograph calibration, and absolute distance measurement [1,2]. Dual-comb spectroscopy (DCS) attracts wide attention because it has various advantages when compared to other techniques in term of the rapid acquisition time, sensitivity, and resolution [3,4]. Dual-comb technique is a type of Fourier transform spectroscopy whereby multi-heterodyne detection is performed using two optical frequency combs with slightly different repetition rate (Δf_{rep}). In these techniques, one comb (signal comb) is transmitted through the sample and it stores the absorption and phase response of atom and molecule in each comb mode. This information is retrieved precisely from an interferogram between the signal comb and the other comb (local comb) precisely without a mechanical moving stage. Owing to its excellent capabilities, several applications DCS have been reported [5–16]. In these studies, the two frequency combs are required to have high mutual coherence and relative stability for high-sensitivity, high-precision, and high-resolution spectroscopy.

The existing dual-comb system uses two independent mode-locked lasers for the generation of two optical frequency combs with a small Δf_{rep}. Since these lasers have independent fluctuations in the free-running state, the interferogram is distorted. Therefore, a tight servo system or signal processing is typically used for high mutual coherence between the two frequency combs. Several schemes have been proposed to overcome this problem [5,6,17–19]. Despite the capabilities of DCS in a wide range of fields, this technique is still mainly restricted to researchers with expertise owing to the high cost of such a system based on two mode-locked lasers and the servo system. Therefore, a simple, robust, and turnkey dual-comb source could offer an alternative solution for a wide range of users, including non-experts.

#362543 https://doi.org/10.1364/OE.27.014648
Journal © 2019 Received 15 Mar 2019; revised 26 Apr 2019; accepted 27 Apr 2019; published 6 May 2019

Optics EXPRESS

Recently, a dual-comb laser, which emits two optical frequency combs from a single-laser cavity with a small Δf_{rep} value, has attracted attention owing to its common-mode noise cancellation and passive mutual coherence. Studies have been performed on dual-wavelength [20], polarization-multiplexed [21], and bidirectional [22,23] mode-locked Er-fiber lasers, an Er-doped ZBLAN chip laser [24], a Kerr-lens mode-locked bidirectional Ti:sapphire laser [25], a mode-locked integrated external-cavity surface emitting laser (MIXSEL) [26], and a microresonator [27]. Although these lasers have excellent capabilities, a dual-comb laser with high practicability and robustness is essential to extend the application of the DCS technique beyond research laboratories.

A fiber-based frequency comb has been widely used as a standard system since it was first reported in the early 2000s [28,29]. Fiber-based frequency combs are inexpensive, compact, and robust owing to their all-fiber-based configuration, and they can generate low phase noise frequency combs [30,31]. Therefore, many dual-comb systems have been reported with two mode-locked fiber lasers. On the contrary, in a single-mode-fiber-based laser cavity configuration, polarization fluctuation can occur due to its high sensitivity to changes in temperature, pressure, and vibration. This could introduce an undesirable instability in the mode-locking operation. Such a fiber-based frequency comb is used in only research laboratories, and it is unsuitable for applications in practical environmental conditions.

To overcome this problem, all-polarization-maintaining (PM) mode-locked fiber lasers have been developed for robustness under all practical environmental conditions [28,32,33]. In these fiber lasers, a semiconductor saturable absorber mirror (SESAM) is used as a mode-locking mechanism. A fieldable DCS system based on two PM fiber lasers was reported by Truong et al. [34]. Using the mode-locking mechanism with SESAMs, an all-PM, polarization-multiplexed, dual-frequency fiber laser was reported by Kolano et al. [35] and Hui [36]. However, owing to the slow relaxation time of a SESAM, the phase noise of fiber-based frequency combs with only SESAM is worse compared to the low phase noise fiber-based frequency combs. Moreover, the relative coherence between the two frequency combs was not investigated.

An all-PM mode-locked Er-fiber laser with a nonlinear amplifying loop mirror (NALM) is an attractive option owing to its low phase noise capability for frequency comb generation [37–40]. In particular, a self-starting all-PM mode-locked fiber laser with NALM and a non-reciprocal phase shifter [41] is more attractive [37,38]. Recently, an all-PM dual-wavelength mode-locked fiber laser with only an NALM has been reported [42]. Owing to the dual-wavelength scheme, the center wavelength of the two outputs are significantly different from each other. Therefore, extra-cavity nonlinear spectral broadening is necessary to overlap their spectra. More importantly, relative coherence in the optical domain between the two outputs has not been demonstrated with the all-PM configuration.

In this study, we develop an all-PM, polarization-multiplexed, dual-comb fiber laser with NALM, which emits two frequency combs with a small Δf_{rep} from a single all-PM fiber laser cavity. Compared with our recent work for a bidirectional dual-comb fiber laser [23], the advantage of the all-PM dual-comb fiber laser is robustness for practical environmental instability. The experimental setup is discussed in the following section. In section 3, the dual-wavelength and single-wavelength polarization-multiplexed mode-locking operations are analyzed. Moreover, the relative coherence between the two outputs is evaluated. In section 4, we summarize and present the conclusion of the study.

2. Experimental setup

Figure 1 shows a schematic of the all-PM, polarization-multiplexed, dual-comb Er-fiber laser, which consists of a linear arm based on free-space and an NALM part. All the fiber components are PM, including the non-doped PMF, Er-doped PMF (PM-EDF, Nufern, PM-ESF-7/125, 1 m), and optical fiber devices. In the fiber components, both polarization axes, i.e., the slow and fast axes in a PMF, are used to generate the two frequency combs. The NALM part consists of

Optics EXPRESS

a 50/50 coupler, two polarization beam combiners (PBCs, extinction ratio of >30 dB), two non-reciprocal phase shifters (NRPSs), and two polarization-maintaining Er-doped fiber amplifiers (PM-EDFAs). A part of the NALM is divided into two paths for both orthogonal polarization axes using the two PBCs. The NRPSs are installed in the separated paths and they assist the self-starting mode-locking operation and generation of low phase noise frequency comb in both the polarization axes. An NRPS consists of two Faraday rotators (FRs), one quarter-waveplate (QWP), and two polarization beam splitters (PBSs, extinction ratio of ~18 dB). A PM-EDFA consists of a PM-EDF, a wavelength division multiplexed coupler, and a 976-nm laser diode. In the linear arm, the two orthogonally polarized beams are divided into two paths through a PBC, and the paths consist of two fiber-optic collimators and two dielectric mirrors. In the cavity configuration, Δf_{rep} can be easily tailored by the path length in the separated region consisting of the fiber and free-space. A 10/90 coupler is also installed in the linear arm, and 10% of the propagating power is coupled out of the cavity via the coupler. All the non-common paths are placed closely such that they share the mechanical vibration. The laser output is divided into two orthogonally polarized beams using a PBC in the output path. The two outputs are measured using an optical spectrum analyzer and a radio-frequency (RF) spectrum analyzer via a fast photodetector. In this setup, since both PMF and PM-EDF have anomalous dispersion at 1550 nm, the net cavity dispersion is also anomalous. In this study, all the experiments are conducted in the free-running operation, as described in the following sections.

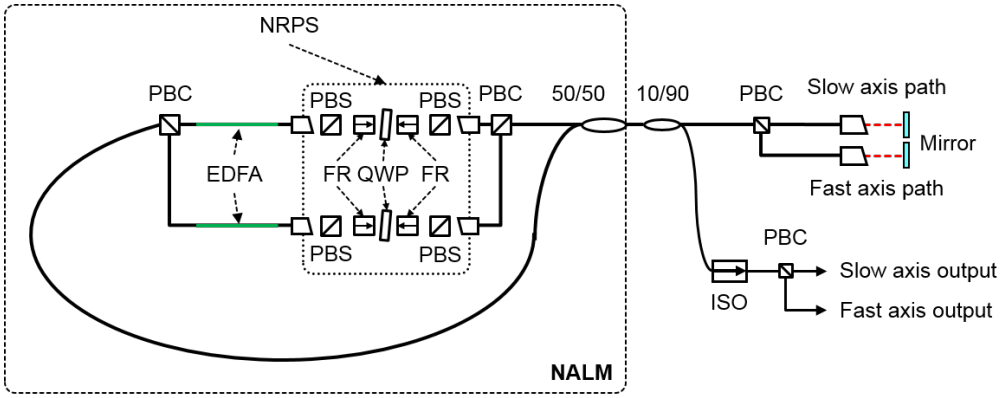

Fig. 1. Schematic of the all-polarization-maintaining, polarization-multiplexed, dual-comb fiber laser with a nonlinear amplifying loop mirror (NALM). PBC: polarization beam combiner; EDFA: Er-doped fiber amplifier; PBS: polarization beam splitter; FR: faraday rotator; QWP: quarter-wave plate; NRPS: non-reciprocal phase shifter; 50/50 and 10/90: 50/50 and 10/90 coupler; ISO: isolator.

3. Experimental results

3.1 Dual-wavelength polarization-multiplexed mode-locking operation

When the pump power is increased, the mode-locking operation is self-started due to the presence of NALM with NRPS. As we decrease the pump power to ~100 mW, we obtain single-pulse mode-locking operation. Figure 2(a) shows the optical spectra of the two orthogonally polarized outputs. In the slow axis output (red curve), the center wavelength is 1564.4 nm, the full-width-at-half-maximum (FWHM) bandwidth ($\Delta\lambda$) of the spectrum is 8.0 nm, and the output power is 0.9 mW. In the fast axis output (blue curve), the center wavelength is 1535.9 nm, $\Delta\lambda$ is 8.0 nm, and the output power is 0.4 mW. Figure 2(b) shows the RF spectra of the two orthogonally polarized outputs at a resolution bandwidth (RBW) of 100 kHz. The repetition rate (f_{rep}) for both the outputs is 21.2 MHz, and Δf_{rep} is 8.9 kHz. Both the f_{rep} values could be varied independently by the position of each collimator in the free-space section of linear arm. Therefore, Δf_{rep} could be conveniently tuned up to ~9 kHz. However, in the current setup, owing to polarization crosstalk between the two orthogonal components in the laser cavity, Δf_{rep} has a

Optics EXPRESS

minimum achievable value. The problem could be solved by improving the polarization extinction ratio of all PMF devices. The center wavelength of the two outputs are significantly different; therefore, the laser operates in the dual-wavelength polarization-multiplexed mode-locking regime at 1564.4 nm and 1535.9 nm simultaneously.

To evaluate the relative stability in the RF domain, we measure f_{rep} for the two combs simultaneously using two frequency counters (Tektronix, FCA3100) with reference to a Rb frequency standard (SRS, FS725). Figures 2(c) and 2(d), respectively, show the temporal variation of f_{rep} for the two outputs and Δf_{rep} in the free-running operation. While both f_{rep} change owing to environmental perturbation, a high relative stability of Δf_{rep} is obtained with a standard deviation of 0.50 Hz (Allan deviation of 0.10 Hz for an averaging time of 1 s) without temperature control, owing to passive common-mode noise cancellation.

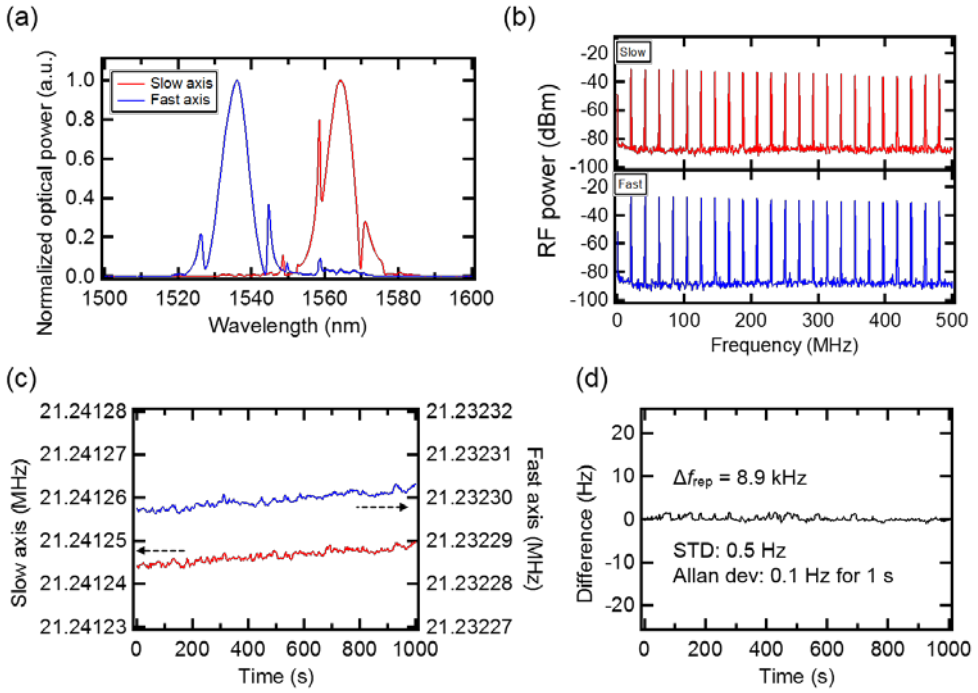

Fig. 2. (a) Optical spectra and (b) RF spectra of the two orthogonally polarized outputs with a dual-wavelength mode-locking operation. Temporal variation of (c) the repetition rates (f_{rep}) of the two outputs and (d) the difference in the repetition rate (Δf_{rep}). "STD" denotes standard deviation; "dev" denotes deviation.

3.2 Single-wavelength polarization-multiplexed mode-locking operation

In the developed all-PM, polarization-multiplexed, dual-comb fiber laser, we can change the center wavelength for mode-locking operation by tailoring the internal cavity loss since the center wavelength with sufficient gain to oscillate also changes. Thus, in practice, by optimizing the fiber coupling alignment after the free-space section in the linear arm, we can realize the single-wavelength operation. In this case, the mode-locking operation is also self-started by increasing the pump power. As we decrease the pump power to ~100 mW, we obtain single-pulse mode-locking operation. Figure 3(a) shows the optical spectra of single-wavelength polarization-multiplexed mode-locking operation. In the slow axis, the center wavelength is 1563.7 nm, $\Delta\lambda$ is 8.2 nm, and the output power is 0.5 mW. In the fast axis, the center wavelength is 1562.7 nm, $\Delta\lambda$ is 8.0 nm, and the output power is 0.5 mW. The spectral shape and Kelly sidebands are different from typical soliton mode-locking owing to miss-alignment for the polarization axis in the non-reciprocal phase shifter. Figure 3(b) shows the

Optics EXPRESS

RF spectra of the two orthogonally polarized outputs at an RBW of 100 kHz. In this case, the f_{rep} value for both the outputs is 22.7 MHz, and Δf_{rep} is 9.5 kHz. Both the f_{rep} values could be varied independently by the position of each collimator in the free-space section of linear arm. Therefore, Δf_{rep} could be conveniently tuned up to ~9 kHz. However, in the current setup, owing to polarization crosstalk between the two orthogonal components in the laser cavity, Δf_{rep} has a minimum achievable value. The problem could be solved by improving the polarization extinction ratio of all PMF devices. As shown in Fig. 3(a), the laser operates in the single-wavelength polarization-multiplexed mode-locking regime. Therefore, the spectra of the two frequency combs overlap without extra-cavity nonlinear spectral broadening.

To evaluate the relative stability in the RF domain, we again measure f_{rep} for the two combs simultaneously using two frequency counters. Figures 3(c) and 3(d), respectively, show the temporal variation of f_{rep} for the two outputs and Δf_{rep} in the free-running operation. While each f_{rep} changes owing to environmental perturbation, a high relative stability of Δf_{rep} is obtained with a standard deviation of 0.50 Hz (Allan deviation of 0.08 Hz for an averaging time of 1 s) without temperature control, owing to passive common-mode noise cancellation. This is a significant advantage for DCS, where Δf_{rep} should be kept constant during multi-heterodyne beat signal measurement. The mode-locking operation can be maintained for one week without realignment or maintenance. Moreover, owing to the all-PM configuration, the mode-locking operation can be maintained in case of any perturbations caused by the touching of the fibers or vibration. f_{rep} can be further increased by reducing the physical length of the cavity. Moreover, we can further stabilize Δf_{rep} by stabilizing the laser cavity, e.g., by temperature control and by introducing an enclosure box.

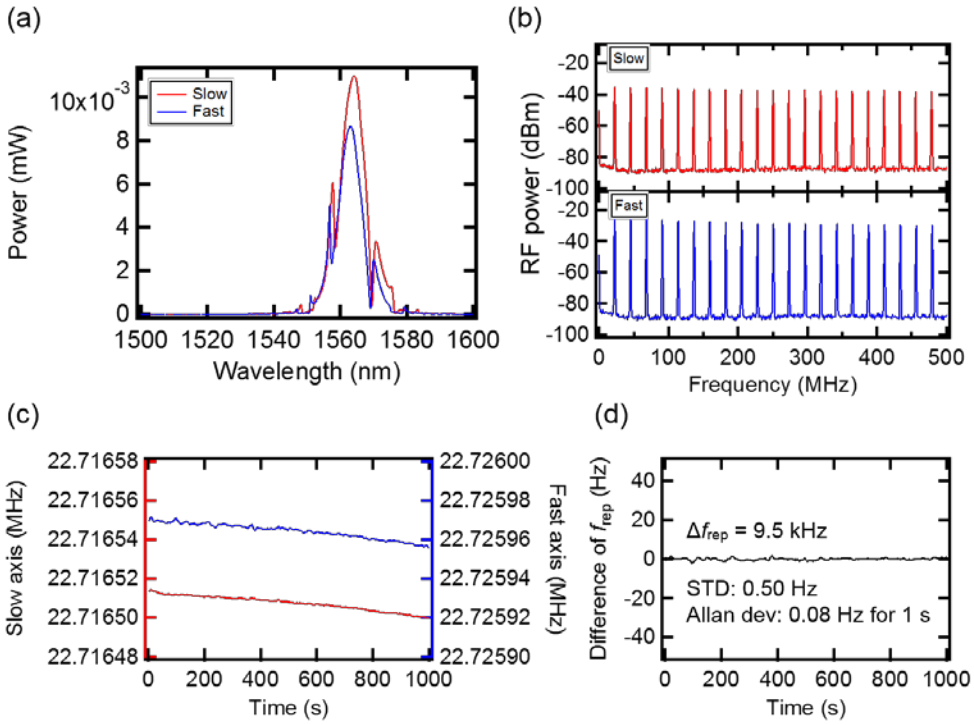

Fig. 3. (a) Optical spectra and (b) RF spectra of the two orthogonally polarized outputs with a single-wavelength mode-locking operation. Temporal variation of (c) the repetition rates (f_{rep}) of the two outputs and (d) the difference in the repetition rate (Δf_{rep}). "STD" denotes standard deviation; "dev" denotes deviation.

Optics EXPRESS

3.3 Evaluation of relative coherence between the two outputs

In this section, we evaluate the relative coherence between the two frequency combs with the same center wavelength.

First, we detect the beat signals between the two outputs and a narrow-linewidth single-frequency laser (Redfern Integrated Optics, RIO ORION laser module) at 1560 nm. Figures 4(a) and 4(b) present the RF spectra of the beat notes for the two frequency combs. We obtain the beat notes with a high signal-to-noise ratio of ~30 dB at an RBW of 100 kHz and a narrow linewidth of ~10 kHz at an RBW of 1 kHz. These results imply that the two orthogonally polarized frequency combs have sufficient coherence at 1560 nm. In addition to the main beat note, a small beat note is also detected with a difference of ~15 dB from the main beat note. This small signal is the beat note between the single-frequency laser and the orthogonally polarized component owing to polarization crosstalk. The crosstalk is due to the PMF devices with a low extinction ratio of ~18 dB which are used in the intra- and extra-laser cavities. In the future, it can be improved using PMF devices with a higher polarization extinction ratio.

Second, to evaluate the relative coherence between the dual outputs of the laser, the two beat notes for both frequency combs are extracted by a low-pass filter and amplified by a low-noise RF amplifier. Then, the two beat notes are mixed with a double-balanced mixer, and the difference frequency signal is extracted by filtering. As shown in Fig. 4(c), the difference frequency beat note has a linewidth of ~1 kHz (for a measurement time of 1.9 ms) in the free-running operation. The result implies that the two frequency combs have high relative coherence. To the best of our knowledge, this is the first demonstration of direct detection of relative beat notes without extra-cavity nonlinear spectral broadening using an all-PM, polarization-multiplexed, dual-comb fiber laser. In the future, all free-space setups can be integrated to further improve the relative stability, and therefore, we expect that multi-heterodyne beat notes between the dual-frequency combs could be detected without such nonlinear spectral broadening.

Optics EXPRESS

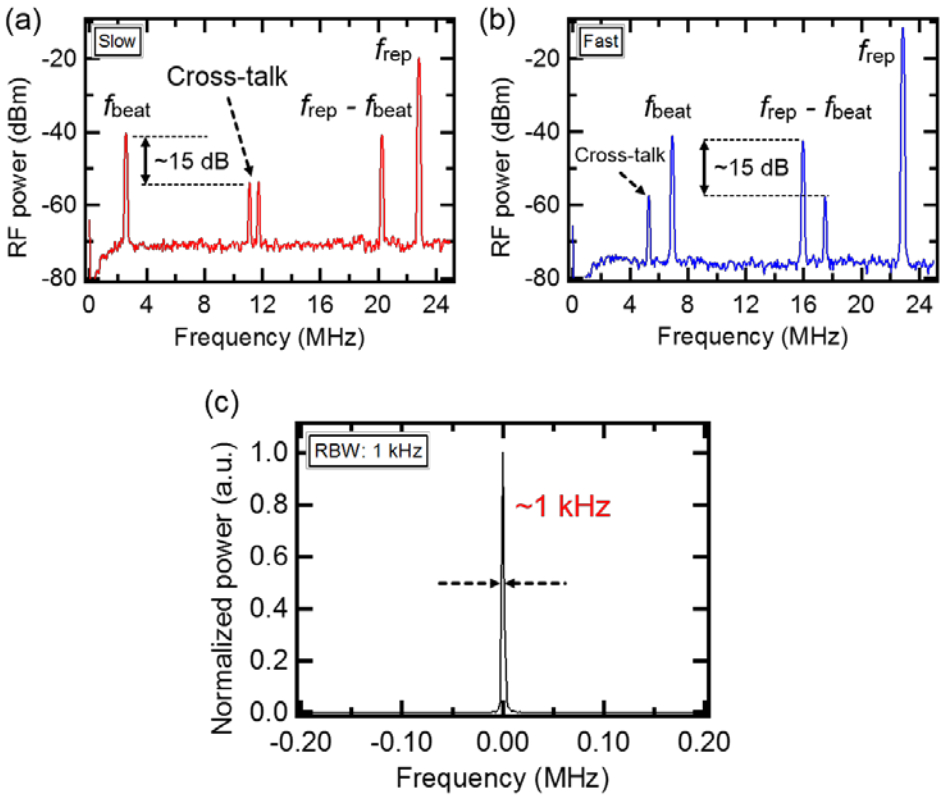

Fig. 4. Beat notes between a narrow-linewidth continuous wave laser and (a) slow, or (b) fast axis outputs. (c) Relative beat note between the dual-frequency combs in optical domain.

4. Conclusion

We developed an all-PM, polarization-multiplexed, dual-comb fiber laser with NALM mode-locking mechanism toward a robust and practical DCS system, which can be used beyond the special laboratories and without the necessity of the expertise in laser stabilization. Owing to polarization-multiplexed mode-locking operation, the dual-frequency combs with Δf_{rep} from the single-laser cavity were generated at the same center wavelength without extra-cavity nonlinear spectral broadening. The two direct outputs from the laser cavity showed broad spectra with an FWHM bandwidth of ~8.0 nm at ~1560 nm. Therefore, we demonstrated the direct detection of the relative beat note between the dual-frequency combs with a linewidth of ~1 kHz in the optical domain. Moreover, a small Δf_{rep} of ~9.5 kHz with a repetition rate (f_{rep}) of ~23 MHz was obtained with a high relative stability in the free-running operation. As these two frequency combs were generated by the same single-laser cavity, the high relative stability and mutual coherence between the two frequency combs were observed owing to passive common-mode noise cancellation. Therefore, multi-heterodyne beat notes is likely to be detected with high visibility without a complex servo system or signal processing between the two frequency combs and/or an extra-cavity nonlinear spectral broadening. Further, the all-PM based configuration is robust to environmental perturbation. In the future, all free-space setups can be integrated to further improve the stability and reduce the size using micro-optic packaging or module. In this laser cavity configuration, the piezo actuators can be installed on two free-space mirrors to stabilize the f_{rep}s, and long-term relative stability can be improved. Therefore, this dual-comb fiber laser can be a powerful tool in practical DCS systems and

Optics EXPRESS

provide a promising alternative to the current systems. Moreover, it can expand the range of applications of optical frequency combs.

Funding

Japan Science and Technology Agency (JST), Exploratory Research for Advanced Technology (ERATO), MINOSHIMA Intelligent Optical Synthesizer (IOS) Project (Grant No. JPMJER1304).

Acknowledgments

We would like to thank Yugo Kusumi (University of Electro-Communications (UEC), Japan) for his assistance in conducting the experiments. We also thank Zheng Zheng (Beihang University, China) for the fruitful discussions, and Akiko Nishiyama (UEC, Japan) and Takeshi Yasui (Tokushima University, Japan) for their valuable advice regarding the DCS system.

Disclosures

The authors declare that there are no conflicts of interest related to this article.

References

1. J. L. Hall, "Defining and measuring optical frequencies: the optical clock opportunity--and more (Nobel lecture)," Rev. Mod. Phys. **78**(4), 1279–1295 (2006).
2. T. W. Hänsch, "Nobel lecture: passion for precision," Rev. Mod. Phys. **78**(4), 1297–1309 (2006).
3. F. Keilmann, C. Gohle, and R. Holzwarth, "Time-domain mid-infrared frequency-comb spectrometer," Opt. Lett. **29**(13), 1542–1544 (2004).
4. I. Coddington, N. R. Newbury, and W. C. Swann, "Dual-comb spectroscopy," Optica **3**(4), 414–426 (2016).
5. S. Okubo, K. Iwakuni, H. Inaba, K. Hosaka, A. Onae, H. Sasada, and F.-L. Hong, "Ultra-broadband dual-comb spectroscopy across 1.0-1.9 μm," Appl. Phys. Express **8**(8), 082402 (2015).
6. A. Nishiyama, S. Yoshida, Y. Nakajima, H. Sasada, K. Nakagawa, A. Onae, and K. Minoshima, "Doppler-free dual-comb spectroscopy of Rb using optical-optical double resonance technique," Opt. Express **24**(22), 25894–25904 (2016).
7. A. Asahara, A. Nishiyama, S. Yoshida, K. I. Kondo, Y. Nakajima, and K. Minoshima, "Dual-comb spectroscopy for rapid characterization of complex optical properties of solids," Opt. Lett. **41**(21), 4971–4974 (2016).
8. A. Asahara and K. Minoshima, "Development of ultrafast time-resolved dual-comb spectroscopy," APL Photonics **2**(4), 041301 (2017).
9. T. Ideguchi, S. Holzner, B. Bernhardt, G. Guelachvili, N. Picqué, and T. W. Hänsch, "Coherent Raman spectro-imaging with laser frequency combs," Nature **502**(7471), 355–358 (2013).
10. A. Nishiyama, Y. Nakajima, K. Nakagawa, and K. Minoshima, "Precise and highly-sensitive Doppler-free two-photon absorption dual-comb spectroscopy using pulse shaping and coherent averaging for fluorescence signal detection," Opt. Express **26**(7), 8957–8967 (2018).
11. Y.-D. Hsieh, Y. Iyonaga, Y. Sakaguchi, S. Yokoyama, H. Inaba, K. Minoshima, F. Hindle, T. Araki, and T. Yasui, "Spectrally interleaved, comb-mode-resolved spectroscopy using swept dual terahertz combs," Sci. Rep. **4**(1), 3816 (2014).
12. N. Kuse, A. Ozawa, and Y. Kobayashi, "Static FBG strain sensor with high resolution and large dynamic range by dual-comb spectroscopy," Opt. Express **21**(9), 11141–11149 (2013).
13. T.-A. Liu, N. R. Newbury, and I. Coddington, "Sub-micron absolute distance measurements in sub-millisecond times with dual free-running femtosecond Er fiber-lasers," Opt. Express **19**(19), 18501–18509 (2011).
14. J. Lee, S. Han, K. Lee, E. Bae, S. Kim, S. Lee, S.-W. Kim, and Y.-J. Kim, "Absolute distance measurement by dual-comb interferometry with adjustable synthetic wavelength," Meas. Sci. Technol. **24**(4), 045201 (2013).
15. S. Han, Y.-J. Kim, and S.-W. Kim, "Parallel determination of absolute distances to multiple targets by time-of-flight measurement using femtosecond light pulses," Opt. Express **23**(20), 25874–25882 (2015).
16. E. Hase, T. Minamikawa, T. Mizuno, S. Miyamoto, R. Ichikawa, Y.-D. Hsieh, K. Shibuya, K. Sato, Y. Nakajima, A. Asahara, K. Minoshima, Y. Mizutani, T. Iwata, H. Yamamoto, and T. Yasui, "Scan-less confocal phase imaging based on dual-comb microscopy," Optica **5**(5), 634–643 (2018).
17. I. Coddington, W. C. Swann, and N. R. Newbury, "Coherent multiheterodyne spectroscopy using stabilized optical frequency combs," Phys. Rev. Lett. **100**(1), 013902 (2008).
18. J. Roy, J.-D. Deschênes, S. Potvin, and J. Genest, "Continuous real-time correction and averaging for frequency comb interferometry," Opt. Express **20**(20), 21932–21939 (2012).
19. T. Ideguchi, A. Poisson, G. Guelachvili, N. Picqué, and T. W. Hänsch, "Adaptive real-time dual-comb spectroscopy," Nat. Commun. **5**(1), 3375 (2014).
20. X. Zhao, G. Hu, B. Zhao, C. Li, Y. Pan, Y. Liu, T. Yasui, and Z. Zheng, "Picometer-resolution dual-comb spectroscopy with a free-running fiber laser," Opt. Express **24**(19), 21833–21845 (2016).

Optics EXPRESS

21. X. Zhao, T. Li, Y. Liu, Q. Li, and Z. Zheng, "Polarization-multiplexed, dual-comb all-fiber mode-locked laser," Photon. Res. **6**(9), 853–857 (2018).
22. S. Mehravar, R. A. Norwood, N. Peyghambarian, and K. Kieu, "Real-time dual-comb spectroscopy with a free-running bidirectionally mode-locked fiber laser," Appl. Phys. Lett. **108**(23), 231104 (2016).
23. Y. Nakajima, Y. Hata, and K. Minoshima, "High-coherence ultra-broadband bidirectional dual-comb fiber laser," Opt. Express **27**(5), 5931–5944 (2019).
24. N. B. Hébert, J. Genest, J.-D. Deschênes, H. Bergeron, G. Y. Chen, C. Khurmi, and D. G. Lancaster, "Self-corrected chip-based dual-comb spectrometer," Opt. Express **25**(7), 8168–8179 (2017).
25. T. Ideguchi, T. Nakamura, Y. Kobayashi, and K. Goda, "Kerr-lens mode-locked bidirectional dual-comb ring laser for broadband dual-comb spectroscopy," Optica **3**(7), 748–753 (2016).
26. S. M. Link, D. J. H. C. Maas, D. Waldburger, and U. Keller, "Dual-comb spectroscopy of water vapor with a free-running semiconductor disk laser," Science **356**(6343), 1164–1168 (2017).
27. A. Dutt, C. Joshi, X. Ji, J. Cardenas, Y. Okawachi, K. Luke, A. L. Gaeta, and M. Lipson, "On-chip dual-comb source for spectroscopy," Sci. Adv. **4**(3), e1701858 (2018).
28. T. R. Schibli, K. Minoshima, F.-L. Hong, H. Inaba, A. Onae, H. Matsumoto, I. Hartl, and M. E. Fermann, "Frequency metrology with a turnkey all-fiber system," Opt. Lett. **29**(21), 2467–2469 (2004).
29. B. R. Washburn, S. A. Diddams, N. R. Newbury, J. W. Nicholson, M. F. Yan, and C. G. Jørgensen, "Phase-locked, erbium-fiber-laser-based frequency comb in the near infrared," Opt. Lett. **29**(3), 250–252 (2004).
30. H. Inaba, Y. Daimon, F.-L. Hong, A. Onae, K. Minoshima, T. R. Schibli, H. Matsumoto, M. Hirano, T. Okuno, M. Onishi, and M. Nakazawa, "Long-term measurement of optical frequencies using a simple, robust and low-noise fiber based frequency comb," Opt. Express **14**(12), 5223–5231 (2006).
31. Y. Nakajima, H. Inaba, K. Hosaka, K. Minoshima, A. Onae, M. Yasuda, T. Kohno, S. Kawato, T. Kobayashi, T. Katsuyama, and F.-L. Hong, "A multi-branch, fiber-based frequency comb with millihertz-level relative linewidths using an intra-cavity electro-optic modulator," Opt. Express **18**(2), 1667–1676 (2010).
32. I. Hartl, G. Imeshev, M. Fermann, C. Langrock, and M. Fejer, "Integrated self-referenced frequency-comb laser based on a combination of fiber and waveguide technology," Opt. Express **13**(17), 6490–6496 (2005).
33. L. C. Sinclair, I. Coddington, W. C. Swann, G. B. Rieker, A. Hati, K. Iwakuni, and N. R. Newbury, "Operation of an optically coherent frequency comb outside the metrology lab," Opt. Express **22**(6), 6996–7006 (2014).
34. G.-W. Truong, E. M. Waxman, K. C. Cossel, E. Baumann, A. Klose, F. R. Giorgetta, W. C. Swann, N. R. Newbury, and I. Coddington, "Accurate frequency referencing for fieldable dual-comb spectroscopy," Opt. Express **24**(26), 30495–30504 (2016).
35. M. Kolano, D. Molter, F. Ellrich, and G. von Freymann, "All-polarization-maintaining, polarization-multiplexed, dual-frequency, mode-locked fiber laser," in Proceedings of 2016 Conference on Lasers and Electro-Optics (CLEO) (IEEE, 2016), pp. 1–2.
36. R. Hui, "Absorption spectroscopy based on polarization-multiplexed dual-frequency femtosecond fiber laser combs," in Conference on Lasers and Electro-Optics, OSA Technical Digest (online) (Optical Society of America, 2017), paper AF1B.2.
37. N. Kuse, J. Jiang, C.-C. Lee, T. R. Schibli, and M. E. Fermann, "All polarization-maintaining Er fiber-based optical frequency combs with nonlinear amplifying loop mirror," Opt. Express **24**(3), 3095–3102 (2016).
38. W. Hänsel, H. Hoogland, M. Giunta, S. Schmid, T. Steinmetz, R. Doubek, P. Mayer, S. Dobner, C. Cleff, M. Fischer, and R. Holzwarth, "All polarization-maintaining fiber laser architecture for robust femtosecond pulse generation," Appl. Phys. B **123**(1), 41 (2017).
39. E. Baumann, F. R. Giorgetta, J. W. Nicholson, W. C. Swann, I. Coddington, and N. R. Newbury, "High-performance, vibration-immune, fiber-laser frequency comb," Opt. Lett. **34**(5), 638–640 (2009).
40. J. W. Nicholson and M. Andrejco, "A polarization maintaining, dispersion managed, femtosecond figure-eight fiber laser," Opt. Express **14**(18), 8160–8167 (2006).
41. H. Lin, D. K. Donald, and W. V. Sorin, "Optimizing polarization states in a figure-8 laser using a nonreciprocal phase shifter," J. Lightwave Technol. **12**(7), 1121–1128 (1994).
42. R. Li, H. Shi, H. Tian, Y. Li, B. Liu, Y. Song, and M. Hu, "All-polarization-maintaining dual-wavelength mode-locked fiber laser based on Sagnac loop filter," Opt. Express **26**(22), 28302–28311 (2018).